Journal of Materials Chemistry A

Accepted Manuscript

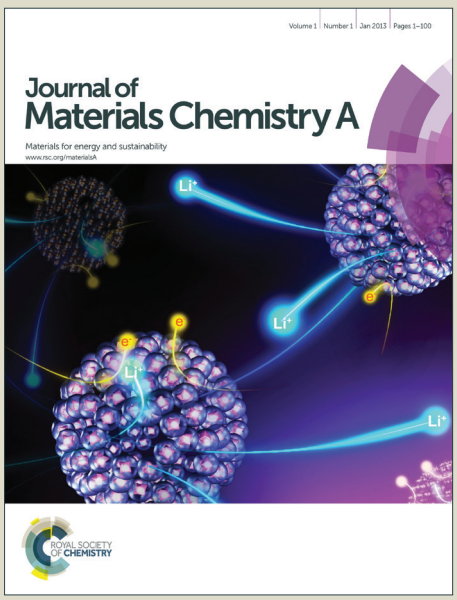

This is an *Accepted Manuscript*, which has been through the Royal Society of Chemistry peer review process and has been accepted for publication.

Accepted Manuscripts are published online shortly after acceptance, before technical editing, formatting and proof reading. Using this free service, authors can make their results available to the community, in citable form, before we publish the edited article. We will replace this *Accepted Manuscript* with the edited and formatted *Advance Article* as soon as it is available.

You can find more information about *Accepted Manuscripts* in the Information for Authors.

Please note that technical editing may introduce minor changes to the text and/or graphics, which may alter content. The journal's standard Terms & Conditions and the Ethical guidelines still apply. In no event shall the Royal Society of Chemistry be held responsible for any errors or omissions in this *Accepted Manuscript* or any consequences arising from the use of any information it contains.

ROYAL SOCIETY OF CHEMISTRY

www.rsc.org/materialsA

CREATED USING THE RSC ARTICLE TEMPLATE (VER. 3.0 OO6)- SEE WWW.RSC.ORG/ELECTRONICFILES FOR DETAILS

ARTICLE TYPE www.rsc.org/xxxxxx | XXXXXXXX

Single porous SnO_2 microtube templated from *Papilio maacki* bristle: new structure towards superior gas-sensing

Wang Zhang,*[a] Junlong Tian,[a] Yu'an Wang,[a] Xiaotian Fang,[a] Yiqiao Huang,[a] Weixin Chen,[a b] Qinglei Liu[a] , and Di Zhang*[a]

Received (in XXX, XXX) Xth XXXXXXXXX 200X, Accepted Xth XXXXXXXXX 200X
First published on the web Xth XXXXXXXXX 200X
DOI: 10.1039/b00000000x

Templated from the bristle on *Papilio maacki* wing, single porous SnO_2 microtube (SPSM) has been synthesized by soakage and sintering. The delicate microstructure and morphology of SPSM were characterized by SEM and TEM. The silver electrodes were precisely contacted on the two ends of SPSM for gas-sensing measurement in the reducing gases. The SPSM was highly sensitive to trace ammonia, formaldehyde, and ethanol at room temperature. It also exhibited low working temperature and short response/recovery time. The average response and recovery time was only about 3s and 30s. Compared with the non-porous structure and the filled structure, the SPSM showed higher sensitivities. The fascinating biomorphic structure of the SPSM will open a new way for the design and application of sensor device for the detection of harmful and toxic gases.

INTRODUCTION

Recently, progress and innovations have been intensely made in studying the gas-sensing of one-dimensional (1D) materials with micro/nanostructures, including nanowire,[1] microtubes on thin films,[2] nanorods,[3] single nanotube,[4] nanobelts,[5] nanograin enchased fibers.[6] These 1D microstructures with high surface-to-volume ratios displayed enhanced and unexpected responses to the chemical molecules. However, sensing performances still have not been adequate in flexibility, operating temperature and response rates. One way to enhance gas adsorption and sensitivity is fabricating tubular materials with pores, like the microtubes with nanopores[7] and porous tubes as humidity sensor.[8] Lee[9] suggested that well-aligned nanoporous structure with high surface area contributes to the rapid and effective gas diffusion, which increases the sensitivity and response speed. Tubes or fibers prepared previously were usually messy networks. The majority of the research were carried on random systems.[10-12] But recent ten years, some self-aligned oxide nanotube layers also has attracted considerable interest. It is furthermore remarkable that this approach is not limited to titanium but can be applied to a large range of other transition metals or alloys to form highly aligned oxide nanotube or pore structures, which will be applied for various applications. [13] Moreover, these aligned oxides could be coated on some devices, such as tiny, vibrating cantilever. In this method, the explosives such as trinitrotoluene binds to the nanotubes array, altering the frequency of the vibration. The device's sensitivity is due to the nanotubes' structure and large surface area.[14]

Some problems such as alignment, separation, and electrical contacts still exist. Single 1D micro/nano materials have aroused great interest and attention. A single one enables us to understand the coupling relationship between structures and properties insightfully without additional and unexpected effects. The electrical conductivity of individual microtube was measured using scanning probe microscope.[15] The conductivity, I-V curve, and magneto resistance of a single microfiber were measured.[16] The transistor devices based on individual microtube yielded a high field-effect mobility.[17] Gas sensor of single nanobelt[18] and nanowire[19, 20] were ever prepared and measured.

In early years, the bristles on butterfly wings were carefully studied. Francisco et al.[21] found that the bristles have hollow interior with some support stalks and regular pores on the wall. The bristles as sensor scales distributed along the margin of the wings were investigated.[22] The bristles, as piliform scales, are high aspect ratio and have some distinct patterns.[23] Meanwhile, the well-organized porous microtube architecture of bristle is based on chitin which is highly hydrophobic.[24] In terms of biological function, the bristles disperse pheromones and scents to transfer information.[25] Consequently, the porous microtube structure and potential sensory function inspired us to fabricate novel sensor materials with delicate structure templated from the original bristles. It goes beyond the limits of traditional technique. Besides, SnO_2, as an n-type semiconducting oxide, was widely used for the detection of gases.[26, 27] combining the sensor material SnO_2 with the complicated porous structure of bristles, sensor materials with high performance could be created.

Here, for the first time, we took advantage of the natural bristles on butterfly wings as bio-template to fabricated gas-sensing materials of SPSM. This microstructure is definitely eye-catching and beautiful. The tubular bristles we used are from *Papilio maacki* wings. Templated from these tubular structures, biomimetic methods [28, 29] were adopted to reproduce these structures. Through chemical dipping and sintering, the sensor materials of SnO_2 microtube, which inherited the microstructure of bristles, were achieved. The method is facile and low-cost compared to other traditional

Journal of Materials Chemistry A Accepted Manuscript

techniques. Later, the SPSM was prepared with electrodes and assembled into a device for gas-sensing measurements. It showed high sensitivities to the low concentration ammonia, formaldehyde, and ethanol at room temperature. The average response and recovery time in the dynamic performance was only about 3s and 30s. Furthermore, we tested the gas sensitivity of the samples based on the three tubular structures (porous, non-porous, and filled) in terms of porosity. The porous type was the microtube with arrayed pores on the wall, namely the SPSM; the non-porous type is the microtube without pores; and the filled type is the solid microfiber. The SPSM with regular pores on the wall displayed the higher sensitivity. The results reported here clearly demonstrate that structure design is significant for the advancement of gas sensor technology.

EXPERIMENTAL METHODS

Synthesis.

The bristles chosen as bio-template came from the male *Papilio maacki* (family *Papiliondae*) (Figure 1a). On the edge of the forewing, the bristles grow densely (Figure 1b). Small-sized (about 5mm × 5mm) wing substances with desired bristles were immersed into diluted hydrochloric acid (adding slight ethanol to increase the wettability of bristles) for 3 hours to get rid of impurities. After that, they were taken out to be rinsed in deionized water and dried. $SnCl_2{\cdot}2H_2O$ powder (3g) was dissolved into ethanol solution (65vol%, 300ml), stirring for 10 hours and subsequently left for 1 day to obtain the yellow Sn-colloid impregnant. Then the bristle templates were dipped in it for 12 hours at 30℃ in sealed vessel. Afterwards, the templates with coating metal ions were rinsed in deionized water, and then placed in the drying oven at 50℃ . Next, the coated bristles were transferred from the wing substance onto the clean cover glass and separated by a thin needle under the microscope. Finally they were heated up to 550℃ in the rate of 1K/min and then kept for 100 minutes in the muffle furnace. Original chitin-based bristles were burnt off, leaving the crystallized SnO_2 with the structure of bristles. Later, the furnace cooled down naturally to room temperature and the final products of "SnO_2 bristles" were achieved. For the gas-sensing tests on three structures, the non-porous and the filled SnO_2 microtubes were also synthesized effectively by adjusting the concentration of the Sn-colloid impregnant (4g $SnCl_2{\cdot}2H_2O$ powder for the non-porous and 5.5g $SnCl_2{\cdot}2H_2O$ powder for the filled). In our research, the supersaturated solution is better for the filled microtube fabrication. The chemical reagents used were not pollutant and the synthesis route was in a low cost as well as environmentally-benign.

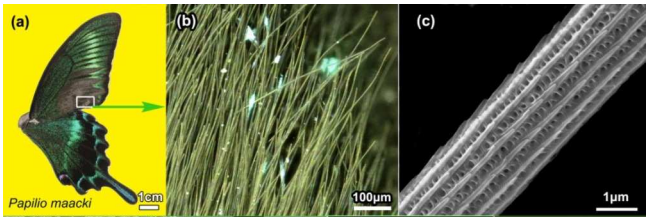

Figure 1. Natural bristles. (a) Photograph of Papilio maacki used in the experiment, the location of bristles on the wing indicated with a rectangle. (b) Densely distributed bristles under optical microscope. (c) SEM image of natural bristle with pores and longitudinal ridges on the wall.

Characterization.

The optical microscope images were taken by KEYENCE super resolution digital microscope VHX-1000. The microstructure and morphology of the original bristles and the final products were investigated by field-emission scanning electron microscope (SEM) which was operated under 5.0 kV (Acc.V). SEM samples were sputtered by a thin gold layer to enhance electrical conductivity before the observation. Transmission electron microscope (TEM) images and selected area electron diffraction (SAED) patterns were obtained on a JEOL JEM-2100F instrument with 200 KV (Acc.V). TEM specimens were prepared by dispersing the products in ethanol and ultrasonic processing for 40 minutes, and picked up onto copper grids.

Measurements of gas-sensing.

After fabricating the porous SnO_2 microtubes separated on the cover glass, conductive silver electrodes were carefully contacted on two ends of the SPSM (Figure 2b) under the optical microscope. Figure 2a gives a vivid illustration of the SPSM contacted with electrodes for gas-sensing. The resistance of silver electrodes is less than 0.01Ω/sq with 12μm thickness while the resistance of the SPSM is up to begohm. Therefore, the resistance of silver electrodes are comparatively low. Then it was placed in an air-tight sensor test chamber with air valves (Figure 2c). The measurements of gas-sensing properties to the low concentration reducing gases (ammonia, ethanol, and formaldehyde) were taken at room temperature (25 ℃). The electrical characteristics were obtained using KEITHLEY 2400 Source Meter (Keithley Instruments, Cleveland, OH). The sample gases with certain concentrations were pumped into the chamber. After the response, the sample gases were cut off and the dry air flowed through the chamber. The sensitivity (S), is defined as $S=(R_a-R_g)/R_g$, where R_a and R_g are the electrical resistance in dry air and in the sample gas, respectively. The resistances were measured under DC voltage of 3V.

Journal of Materials Chemistry A Accepted Manuscript

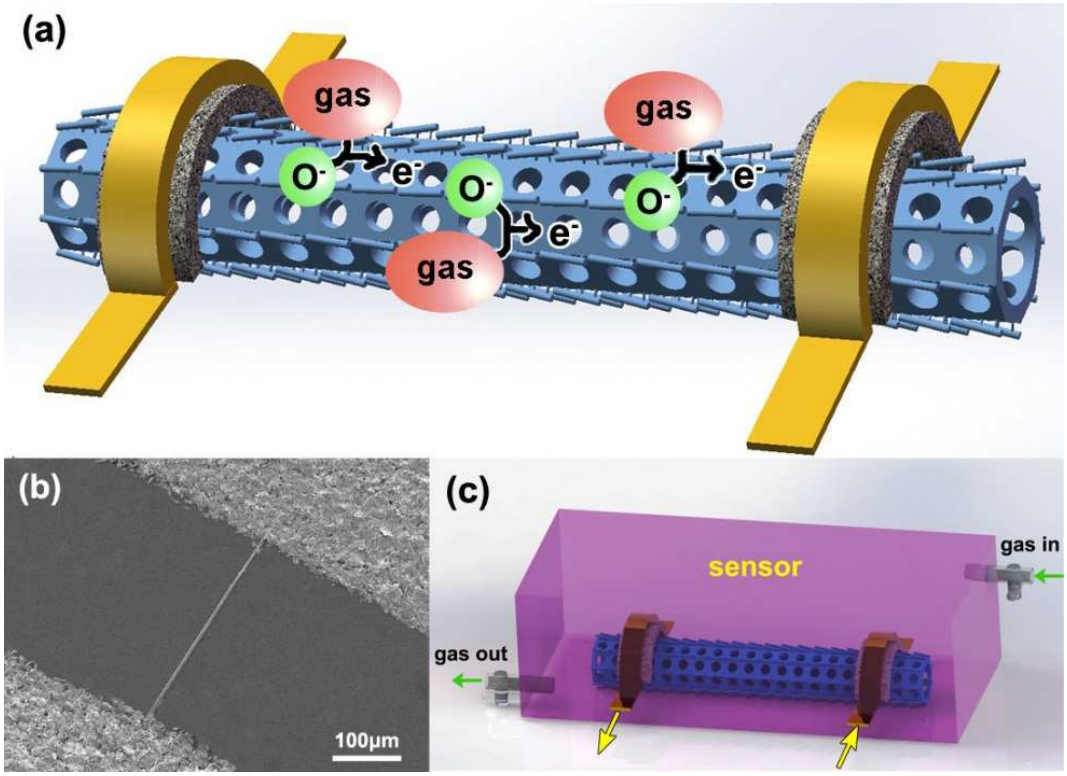

Figure 2. Set up for measuring sensing characteristics of the SPSM at room temperature. (a) Schematic view of the SPSM connected with electrodes for gas-sensing. (b) SEM image of the SPSM connected with conductive silver paste, the spacing is about 300μm. (c) Device for the gas-sensing measurements of the SPSM, gases and dry air flow through the air-tight chamber.

RESULTS AND DISCUSSION

Characterization of porous SnO_2 microtube.

The natural bristles are densely distributed on *Papilio maacki* wing (Figure 1b). It is estimated to have 500 bristles per square centimeter and the total area covered by bristles is 8 cm^2 on the wing. This enabled us to fabricate nearly 4000 "SnO_2 bristles" at a time from one wing. The natural bristles are hollow and porous tubes, about 2μm in diameter, with pores regularly distributed on the wall (Figure 1c). In the final products of SnO_2, the porous and tubular structure was excellently retained (Figure 3a and 3b). On the wall of SnO_2 microtube, the longitudinal ridges and sequential pores are regularly distributed. The SnO_2 microtube was relatively long and straight with high length-diameter ratio. This character is conducive to prepare the SPSM sensor device. Figure 3b shows a portion of the SPSM with the magnified wall and cross section. The ordered pores on the wall were all kept well, perfectly inheriting the microstructure of natural bristle. All these demonstrated that the porous SnO_2 microtube could be extraordinary and novel materials for developing gas sensor.

TEM further revealed the morphology of the microtube. Figure 3c shows the SPSM with the morphology of porous wall. The SAED pattern (inset in Figure 3c) demonstrates that the biomorphic SnO_2 is polycrystalline, and rings indexed to (2 1 1), (1 0 1), (1 1 0) and (3 1 0) diffraction, respectively. The high porosity of the SPSM is demonstrated in Figure 3d. The pores on the bottom side can be seen through the pores on the upper side, which indicates the hollow and porous tubular structure.

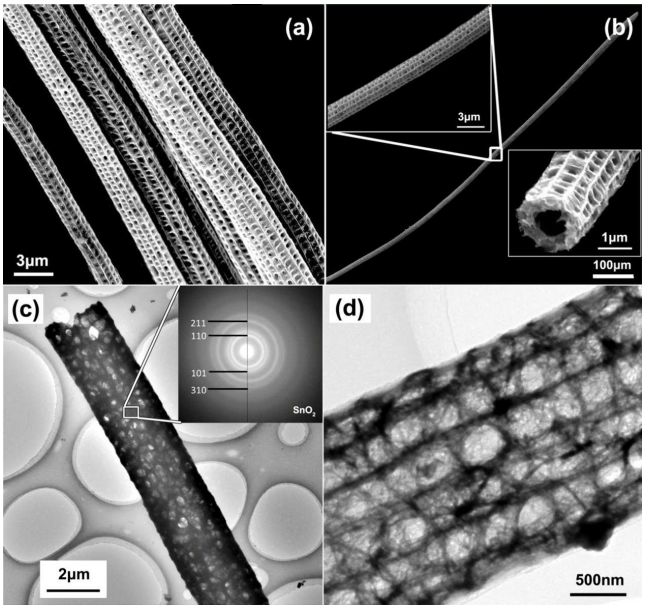

Figure 3. SEM and TEM images of the fabricated SnO_2 microtube. (a) A bunch of SnO_2 microtubes. (b) A long SPSM, up to 1mm in length, and the inserts show its magnified wall and cross-section. (c) The morphology of SnO_2 microtube and the corresponding SAED pattern. (d) The enlarged SnO_2 microtube with legible pores.

Journal of Materials Chemistry A Accepted Manuscript

Gas-sensing measurements.

After fabricating the SPSM, its gas-sensing properties were explored with the sensor device in Figure 2c. When low concentration sample gases filled the closed chamber, the resistance of the SPSM decreased sharply. When the dry air flushed through to dilute the gas concentration, the resistance soon increased up to the original. To the different concentrations of gases, the S varied and positively correlated. The three kinds of gases we studied are representative and significant in the gas detection. Ethanol gas sensor is applied in automobile industry, detecting the alcohol content to avoid accidents. Ammonia, the colorless toxic gas with pungent smell, has extensive industrial and agriculture application but also does harm to people's health. Formaldehyde is one of the main indoor air pollutants, which seriously threatens human body. These three gases are all reducing gases, among which formaldehyde is strongly reducing, especially.

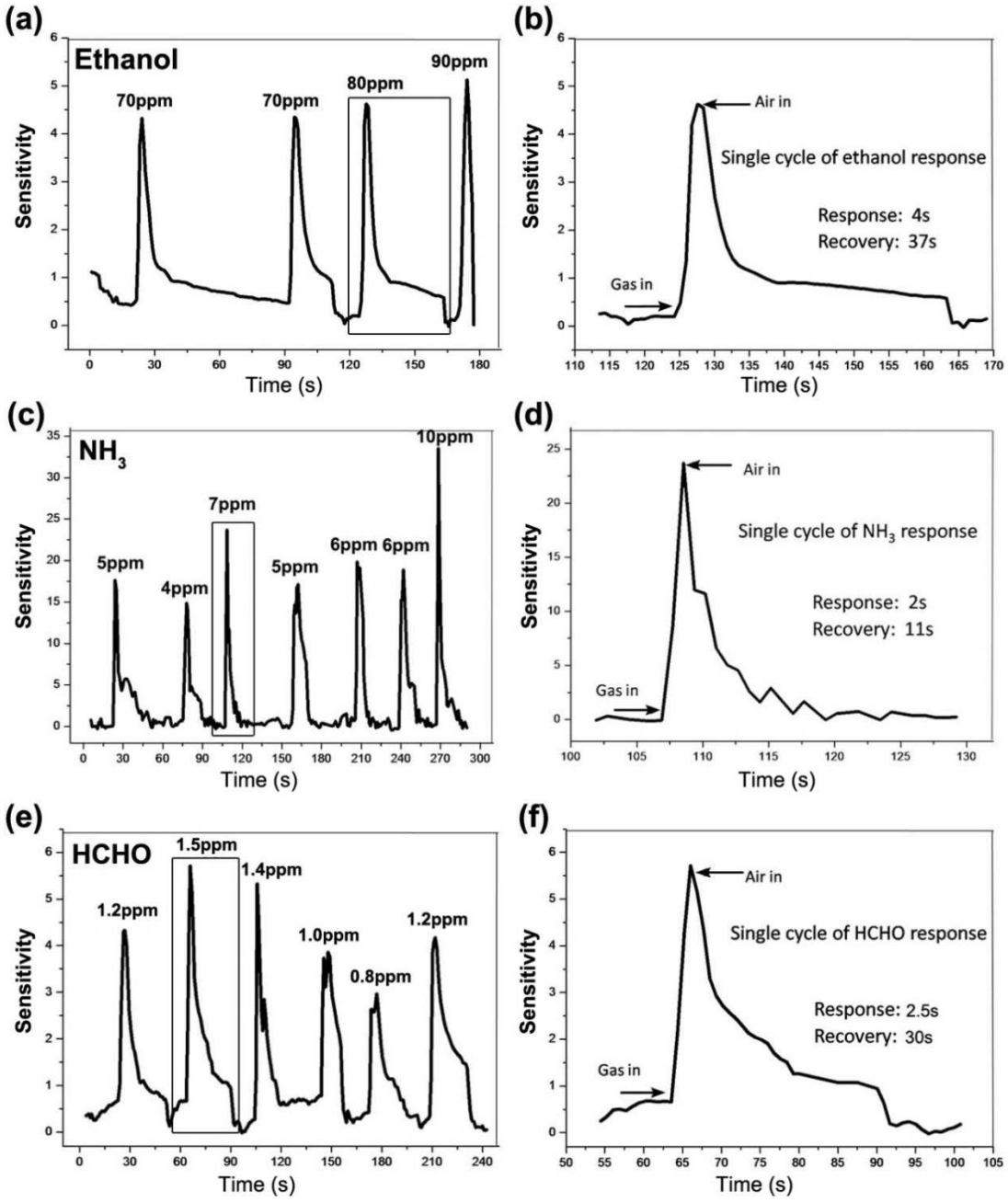

Figure 4. Dynamic gas-sensing response of the SPSM for room-temperature detections of ethanol (a, b), ammonia (c, d), formaldehyde (e, f). In the enlarged single cycles (b, d, and f), the response/recovery time is indicated.

Journal of Materials Chemistry A Accepted Manuscript

The SPSM sensor showed the reliability in detecting the same concentration sample gases, and discrimination to the slight difference of concentration. In Figure 4e, the SPSM sensor responded to 1.2ppm formaldehyde stably, and varied the S to different concentrations (0.8ppm, 1.0ppm, 1.2ppm, 1.4ppm, and 1.5ppm). To the 0.8ppm formaldehyde, S was 3; when up to 1.5ppm, S was about 5.5. Such reproducibility and sensitivity were also demonstrated in ethanol and ammonia (Figure 4a and 4c). The S was high to quite low concentration ammonia and formaldehyde. Notably, the S reached about 33 to 10ppm ammonia (Figure 4c), and 5.7 to 1.5ppm formaldehyde (Figure 4e). The large surface-to-volume ratio of the SPSM leaded to the performance that tiny change in the environment could trigger a detectable response to just few molecules.

The average response and recovery time to the three gases were only about 3s and 30s. Especially, to ammonia, the average response/recovery time during the whole cycle was about 2s and 15s. One of its cycles is magnified to clearly show the short response/recovery time (Figure 4d). For the other two gases, the corresponding response/recovery time is showed in Figure 4b and Figure 4f. It was reported that well-defined pore architectures induce the ultrafast gas response kinetics.[9] Here it is the pores on the SPSM that promote the response/recovery rate.

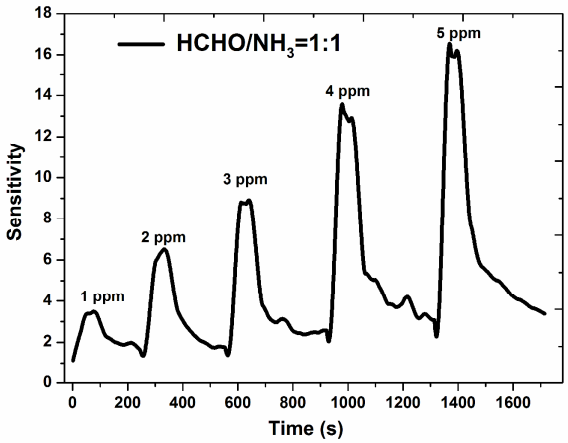

Figure 5. Dynamic gas-sensing response of the SPSM for room-temperature detections of the mixture gas.

At room temperature, it is quite attractive to have such high S and the fast response. By comparison, it is superior to the gas-sensing properties of some nanowires and nanotubes,[30] hierarchical flowerlike nanostructure,[31] and carbon/silicon heterojunctions[32] at room temperature reported before. Commercial and industrial applications require the gas sensors to be operated at lower temperature (especially at room temperature) to increase the robustness and life of sensor. For the flammable and explosive gases, detection also has to be taken at lower temperature. Researches on developing sensors operated at low temperature were reported.[33, 34] However, those sensor materials are in nano-scale with challenging fabrication and assembling. Here the SPSM sensor is more feasible in manufacturing as it is up to micro-scale.

Comparatively, the SPSM was more sensitive to ammonia and formaldehyde. This could be due to the high chemical reducibility of the two gases. Therefore, it exhibits an additional advantage of selectivity, which can still be further studied by molecular design or doping. Moreover, in regard to the limit of detectable concentration of formaldehyde, the SPSM sensor is remarkable. Small amount of formaldehyde (0.8ppm) was still detectable (Figure 4e). Moreover, the combination sensitivity was also tested in a reconstituted air (Figure 5). Though no special selectivity performance was shown, only normal linear superposition relationship was given out. The existence of ammonia will enhance the intensity of the sensitivity compared to formaldehyde. This character is very important and useful in sensing formaldehyde, ammonia or the combination of the two (in most cases) which does great damage to our health. American Conference of Governmental Industrial Hygienists (ACGIH) reported that the threshold limit value of formaldehyde in occupational exposure is 0.3ppm. Therefore, the low limit of detectable concentration of the SPSM sensor is of great significance for the health monitoring. Along with the increasing attention to the environmental pollutions and human health, detection of the trace gas pollutants in the air is necessary and urgent.

Comparison of the three structures.

The gas-sensing tests were taken on the three different kinds of SnO_2 microtubes we prepared. They are porous, non-porous, and filled tubular structures, respectively (Figure 6a, 6b, and 6c). Their lengths and external diameters are almost the same. The porous SnO_2 microtube (the SPSM) has regular pores arranging along the wall, which provides numerous channels interconnecting outer and inner layers of the tube for the gas diffusion. The non-porous one is hollow without pores on the wall, greatly closing the channels of outer and inner layers. The filled one acts like a solid fiber. The minimum weight for the N_2 adsorption test for the surface area will be more than 50 mg taking Micromeritics' ASAP 2020 as an example. So it will be very tough for us to meet the requirements for the test by collection these single tubes as much as possible. Based on the observation and measurements on these samples by SEM and TEM, we estimated the surface area as 271.1 m^2/g, 143.8 m^2/g, 130.4 m^2/g for porous microtube, non-porous microtube and filled respectively.

Among the three strucutres, the SPSM has the largest specific surface area. Figure 6d shows the dynamic sensing test results on the three structures for formaldehyde with increasing gas concentration. At each specific gas concentration, the sensitivity is porous > non-porous > filled. It confirmed that the porous and hollow structure is conducive to improve the gas-sensing performance. When the structure is non-porous, the inner surface is not sufficiently exposed. When it is filled structure, only the outside surface region contributes to the gas-sensing reaction while the internal part is inactive. The higher S achieved using porous nanostructure is in accordance with that of the hierarchical hollow SnO_2 spheres[35] which showed higher gas response than the dense microspheres.

Figure 7 reveals the S on the dependence of gas concentrations to the three kinds of tubular structures for

Journal of Materials Chemistry A Accepted Manuscript

ethanol, ammonia, and formaldehyde, respectively. The relationship of S: porous > non-porous > filled, was demonstrated in all three gases. The relationship between sensitivity and gas concentration before reaching the saturation of gas-sensing is almost linear, which is helpful for the application of digitized gas sensor. The linear relationship with gas concentration in the measured range was also found in the SnO_2 nanowires sensor[36] that responded to liquefied petroleum gas and NH_3.

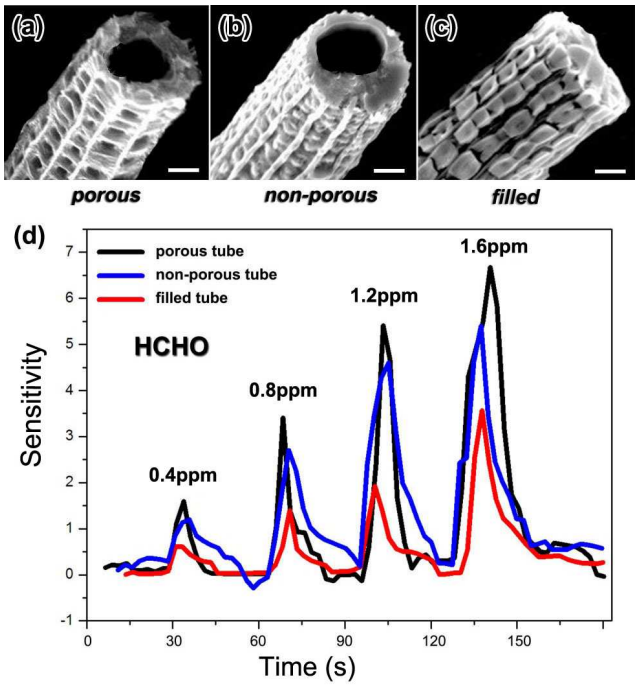

Figure 6. (a-c) SEM of the three tubular structures for comparison: (a) porous tube with pores on the wall, (b) non-porous tube without pores, (c) filled tube without hollow structure, scale bar: 500nm. (d) The dynamic gas-sensing performance of the three structures to formaldehyde with increasing gas concentration.

In addition to the surface area, it is deduced that the effective diffusion such as Knudsen diffusion will play a key role in the gas diffusion as sensor process. According to the classic free mean paths of the gas molecules (FMP) formula

$$\bar{\lambda}=\frac{k_B T}{\sqrt{2}\pi d^2 p}$$

where k_B is the Boltzmann constant in J/K, T is the temperature in K, p is pressure in Pascals, and d is the diameter of the gas particles in meters.

The FMP of NH_3, HCHO and C_2H_5OH are estimated as 46.37nm, 36.56nm and 25.39nm, which are roughly comparable to the pore size on the microtubes. Diffusion is then predominantly described by Knudsen diffusion[37], where the diffusion coefficient D_k is linearly related to the pore width r:

$$D_k = 4r/3 \sqrt{(2RT)/\pi M}$$

(M is the molecular mass of the gas molecule; R and T are the universal gas constant and temperature, respectively.)

This study also showed that the diffusion coefficient is one order of magnitude higher than for non-ordered silica material. It suggests that for sensing purposes the ordered, mesoporous material may be expected to result in faster response and regeneration times

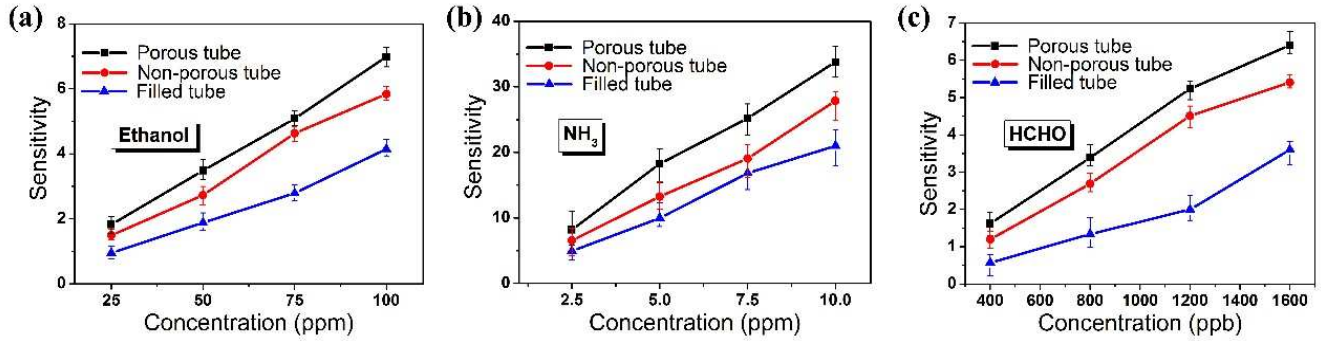

Figure 7. The S to ethanol (a), ammonia (b), and formaldehyde (c) on the dependence of gas concentrations in terms of the three kinds of tubular structures.

Effects of the structure on gas-sensing.

Based on the model of depletion layer modulation by oxygen absorption,[38] oxygen from the ambient is broadly adsorbed on the surface of the SPSM and extracts electrons from the SnO_2 conduction band after ionizing into O^-. It causes the carrier concentration and electron mobility to decrease. With the regular meso pores, the reducing gas molecules are easier to contact with the inner wall of the microtube through the large amounts of pores as channels. When they react with the adsorbed O^-, both the carrier concentration and electron mobility of SnO_2 largely increase after releasing the trapped electron back to the conduction band. Because gas can freely and efficiently enter and leave through the network of pores (Figure 8), the entire sensing surfaces take an active part in the gas-sensing performance. Besides, the longitudinal ridges on the wall of the SPSM provide additional chemically reactive sites for the gas molecules when they gather along the two sides. Consequently, the SPSM effectively adsorbs more gas molecules, promotes fast gas diffusion, and thus achieves high gas sensitivities with short response and recovery time even at room temperature.

Journal of Materials Chemistry A Accepted Manuscript

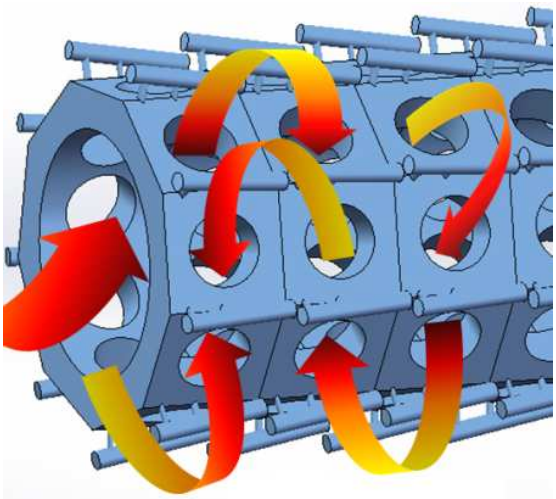

Figure 8. Diagram of the gas transportation on the SPSM.

CONCLUSIONS

In this work, the porous and biomorphic SnO_2 microtube templated from the *Papilio maacki* bristle was synthesized by chemical soakage in the Sn-colloid impregnant and subsequent sintering. The SPSM with electrodes contacted on two ends was assembled into the gas sensor device. It was highly sensitive to low concentration ammonia, formaldehyde, and ethanol at room temperature. The short response/recovery time and low working temperature are quite attractive. The porous bristle structure of the SPSM contributes to the superior gas-sensing performance with the large reactive area and efficient diffusion channels. The SPSM will be the optimal function component for miniature sensor devices in practical applications. Furthermore, it is going to spark inspirations for the continuing exploration and real breakthrough of nanomaterial sensing mechanism.

Acknowledgements

This work was supported by the National Natural Science Foundation of China (no. 51202145, no. 51131004, no. 51001070 and no. 51171110), the National Basic Research Program of China (973 Program, no. 2011cb922200). Research Fund for the Doctoral Program of Higher Education of China (20120073120006 and 20120073130001), and Scientific Research Foundation for Returned Scholars.

Notes and references

[a] *State Key Laboratory of Metal Matrix Composites, Shanghai Jiao Tong University, Shanghai, 200240, People's Republic of China. Fax: +86-21-3420-2749; Tel: +86-21-3420-2634; E-mail: wangzhang@sjtu.edu.cn; dizhang@sjtu.edu.cn*

[b] Department of Materials Science and Engineering, University of Wisconsin-Madison, Madison, Wisconsin 53706, USA

1. F. Yang, K. C. Donavan, S.-C. Kung and R. M. Penner, *Nano Lett.* , 2012, **12**, 2924-2930.
2. P. Ma, Y. Chen, Y. Bian and J. Jiang, *Langmuir*, 2009, **26**, 3678-3684.
3. P. Gunawan, L. Mei, J. Teo, J. Ma, J. Highfield, Q. Li and Z. Zhong, *Langmuir*, 2012, **28**, 14090-14099.
4. Y. Liu and M. Liu, *Adv Funct Mater*, 2005, **15**, 57-62.
5. P. Hu, G. Du, W. Zhou, J. Cui, J. Lin, H. Liu, D. Liu, J. Wang and S. Chen, *ACS Appl. Mat. Interfaces* 2010, **2**, 3263-3269.
6. J. Gong, Y. Li, Z. Hu, Z. Zhou and Y. Deng, *The Journal of Physical Chemistry C*, 2010, **114**, 9970-9974.
7. W. Zhang, D. Zhang, T. Fan, J. Ding, Q. Guo and H. Ogawa, *Nanotechnology*, 2006, **17**, 840.
8. H. Yin, K. Yu, H. Peng, Z. Zhang, R. Huang, J. Travas-Sejdic and Z. Zhu, *J Mater Chem*, 2012, **22**, 5013-5019.
9. J.-H. Lee, *Sens. Actuators, B* 2009, **140**, 319-336.
10. P. Offermans, M. Crego-Calama and S. H. Brongersma, *Nano Lett.* , 2010, **10**, 2412-2415.
11. P.-C. Chen, S. Sukcharoenchoke, K. Ryu, L. Gomez de Arco, A. Badmaev, C. Wang and C. Zhou, *Adv Mater*, 2010, **22**, 1900-1904.
12. X. Lai, D. Wang, N. Han, J. Du, J. Li, C. Xing, Y. Chen and X. Li, *Chem Mater*, 2010, **22**, 3033-3042.
13. P. Roy, S. Berger and P. Schmuki, *Angewandte Chemie International Edition*, 2011, **50**, 2904-2939.
14. D. Spitzer, T. Cottineau, N. Piazzon, S. Josset, F. Schnell, S. N. Pronkin, E. R. Savinova and V. Keller, *Angewandte Chemie International Edition*, 2012, **51**, 5334-5338.
15. S. Xiong, Q. Wang and Y. Chen, *Mater Lett*, 2007, **61**, 2965-2968.
16. Y. Long, K. Huang, J. Yuan, D. Han, L. Niu, Z. Chen, C. Gu, A. Jin and J. L. Duvail, *Appl Phys Lett*, 2006, **88**, 162113.
17. D. H. Kim, D. Y. Lee, S. G. Lee and K. Cho, *Chem Mater*, 2012.
18. L. Fields, J. Zheng, Y. Cheng and P. Xiong, *Appl Phys Lett*, 2006, **88**, 263102-263102-263103.
19. F. Hernandez-Ramirez, S. Barth, A. Tarancon, O. Casals, E. Pellicer, J. Rodriguez, A. Romano-Rodriguez, J. R. Morante and S. Mathur, *Nanotechnology*, 2007, **18**, 424016.
20. L. Mai, L. Xu, Q. Gao, C. Han, B. Hu and Y. Pi, *Nano Lett.* , 2010, **10**, 2604-2608.
21. F. Hernández-Chavarría, A. Hernández and A. Sittenfeld, *Rev Biol Trop*, 2004, **52**, 919-926.
22. A. Yoshida and J. Emoto, *Ann Entomol Soc Am*, 2010, **103**, 988-992.
23. V. R. Binetti, J. D. Schiffman, O. D. Leaffer, J. E. Spanier and C. L. Schauer, *Integr. Biol.* , 2009, **1**, 324-329.
24. M. N. V. Ravi Kumar, *React. Funct. Polym.* , 2000, **46**, 1-27.
25. H. Ghiradella, in *Adv Insect Physiol*, eds. C. Jérôme and J. S. Stephen, Academic Press, 2010, vol. Volume 38, pp. 135-180.
26. F. Gyger, M. Hu□bner, C. Feldmann, N. Barsan and U. Weimar, *Chem Mater*, 2010, **22**, 4821-4827.
27. P. Manjula, R. Boppella and S. V. Manorama, *ACS Appl. Mat. Interfaces* 2012.
28. C. Sanchez, H. Arribart and M. M. Giraud Guille, *Nat Mater*, 2005, **4**, 277-288.
29. B.-L. Su, C. Sanchez and X.-Y. Yang, *Hierarchically Structured Porous Materials*, Wiley. com, 2012.
30. Z. Wang, L. Wang, J. Huang, H. Wang, L. Pan and X. Wei, *J Mater Chem*, 2010, **20**, 2457-2463.
31. H. Wang, J. Gao, Z. Li, Y. Ge, K. Kan and K. Shi, *CrystEngComm*, 2012, **14**, 6843-6852.
32. Q. Xue, H. Chen, Q. Li, K. Yan, F. Besenbacher and M. Dong, *Energy Environ. Sci.* , 2010, **3**, 288-291.

Journal of Materials Chemistry A Accepted Manuscript

33. G. Lu, L. E. Ocola and J. Chen, *Adv Mater*, 2009, **21**, 2487-2491.
34. N. Du, H. Zhang, B. D. Chen, X. Y. Ma, Z. H. Liu, J. B. Wu and D. R. Yang, *Adv Mater*, 2007, **19**, 1641-1645.
35. H.-R. Kim, K.-I. Choi, J.-H. Lee and S. A. Akbar, *Sens. Actuators, B* 2009, **136**, 138-143.
36. L. V. Thong, L. T. N. Loan and N. Van Hieu, *Sens. Actuators, B* 2010, **150**, 112-119.
37. T. Wagner, S. Haffer, C. Weinberger, D. Klaus and M. Tiemann, *Chem Soc Rev*, 2013, **42**, 4036-4053.
38. P. Sun, W. Zhao, Y. Cao, Y. Guan, Y. Sun and G. Lu, *CrystEngComm*, 2011, **13**, 3718-3724.

Journal of Materials Chemistry A Accepted Manuscript